Research paper

WOA-based Interval Type II Fuzzy Fractional-order Controller Design for a Two-Link Robot Arm

F. Jamshidi[1], M. Vaghefi[2,*]

[1]Department of Electrical Engineering, Faculty of Engineering, Fasa University, Fasa, Iran.

[2]Department of Electrical Engineering, Islamic Azad University, Shiraz Branch, Shiraz, Iran.

Article Info

[*]Corresponding Author's Email Address:
mahsavaghefi@gmail.com

Abstract

Background and Objectives: A robot arm is a multi-input multi-output and non-linear system that has many industrial applications. Parameter uncertainties and external disturbances attenuate the performance of this system and a controller design is hence necessary to overcome them.

Methods: In this paper, the interval Type II Fuzzy fractional-order proportional integral differential (IT2FO-FPID) controller is designed to control a robot arm with 2 degrees of freedom (two-link robot arm). Whale optimization algorithm (WOA) is used to determine the optimal value of controller parameters. The performance of IT2FO-FPID is compared with PID, fractional-order PID (FOPID) and Fuzzy FOPID whose parameters are determined by WOA. The performance of IT2FO-FPID whose parameters are determined by WOA, genetic algorithm, and particle swarm optimization methods are compared.

Results: Quantitative and qualitative results of simulations indicate performance improvement with the IT2FO-FPID controller. The ability of WOA in optimizing the parameters of the IT2FO-FPID controller is demonstrated.

Conclusion: Sensitivity analysis and the study of the effect of parameter variations and disturbances confirm the robust performance of WOA-based IT2FO-FPID.

Introduction

Researchers are interested in the control of a robot arm because of its widespread use in industries, nuclear processes, and medical plans, especially for tracking purposes. Some efforts have been made to accurately control the movement of the robot. As an instant, in [1], the problem of minimizing moving parts of a given robot arm for positioning its end effector at a given target point as well as minimizing the movement of the movable parts was considered. The robot arm model is nonlinear and has uncertainties and unmodeled dynamics [2]. The proportional integral derivative (PID) controller is the most applicable industrial controller due to its ease of design, implementation, and tuning. Most controllers used in the industry have either PID or PID structure used in their design [3]. In recent years, the application of the Fuzzy logic to control the nonlinear systems and perturbed systems with unstructured uncertainties has been increased. The fuzzy controller is recommended because of its unique features such as applying expert human knowledge and inexpensive maintenance costs [4].

In [5], using the Lyapunov's theorem, a self-tuning Fuzzy PID controller was presented for the robot arm, whose performance was better than the classic PID controller. In [6], a type II Fuzzy PID controller was offered for the robot arm, which is more robust than the type I fuzzy controllers. In [7], a robot physically like the snake was modeled; to achieve control objectives such as tracking the speed and angle of motion. A sliding mode controller (SMC) was designed; Lyapunov's theorem was applied to obtain control parameters to ensure robust stability. In [8], a combination of neural networks and adaptive SMC was used to control a two-arm robot. First, the neural network estimates the dynamic of the system. Then, the SMC controls it. Neural network weights are determined via the particle swarm optimization (PSO) algorithm.

In recent years, the application of fractional-order calculus in controller design has been increased due to their more degrees of freedom and greater flexibility. In [9], combining fractional-order calculus and the classic PID, a fractional-order PID (FOPID) controller was proposed. Researches showed the outperformance of the FOPID controller in comparison to the PID controller. In [10], the FOPID controller was designed for a robot arm with two degrees of freedom (two-link robot arm), which was highly robust, self-tuning and superior to the PID controller. A combination of a Fuzzy system and a FOPID controller, called FO-FPID, was presented in [11]. FO-FPID controller controls the nonlinear and time-delay systems appropriately. In [12], numerical simulations demonstrated that the optimized FO-FPID controller significantly outperforms FO-FPID, FPID, and PID controllers. In [13], a PID controller was designed for the robot arm; the integer-order derivative and integrator was replaced by the fractional-order derivative and integrator, respectively. The controller parameters were determined using the Cuckoo search algorithm (CSA) to minimize the magnitude of the tracking error. It was shown that the CSA-based FOPID controller is robust against parameter variations and can attenuate disturbances. In [14], a controller similar to [13] was designed; the type I Fuzzy system (T1FS) was substituted with type II Fuzzy system (T2FS); the controller parameters were determined with the aim of minimizing the absolute of the tracking error and the square of the control effort using a new combination of GA and the artificial bee colony (ABC) algorithm. It was shown that the controllers [13] and [14] are robust against the variations of the parameters and can eliminate disturbances very well. In [15], an FO-FPID controller was designed to control the position of the rigid two-link robot arm, and trace the path, and its parameters were adjusted using the CSA. It was shown that CSA has a higher convergence rate than PSO and GA and converges to a lower value of the cost function, in this problem.

In [16], a meta-heuristic optimization algorithm inspired from nature was introduced. It is referred to as the Whale optimization algorithm (WOA) and mimics the social behavior of the humpback whales. The simulation results showed that this algorithm has a high competitive power compared to the other meta-heuristic algorithms in solving different optimization problems. In this paper, for controlling a two-link robot arm, one Fuzzy PID controller is designed for each link to track the desired reference position. T2FS is used because of its merit in controlling the systems. The interval type II Fuzzy system (IT2FS) is a special kind of the T2FS with much less calculation volume and favorable abilities to cope with uncertainties in various applications. WOA is used to optimize the value of the parameters of the proposed controller.

The organization of the paper is as follows. In the next section, the mathematical model of the two-link robot arm is derived. In the third Section, the fractional-order controller and IT2FS are described and the proposed controllers are designed. WOA is introduced in the fourth Section. In Section 5, the simulation results are discussed and the performance of the designed controllers is qualitatively and quantitatively compared. Finally, Section 6 concludes this paper.

Mathematical Model of a Two-Link Arm Robot

In this paper, controlling a two-link robot arm, as shown in Fig. 1, is considered. A mathematical model describing the dynamic behavior of a system is required to design a controller. The kinetic and potential energies of the robot are calculated. Using the Lagrangian motion equations, the robot model is obtained. $q = [\theta_1, \theta_2]^T$ is the position vector of the robot, and $\tau = [\tau_1, \tau_2]^T$ is its force vector generated by a motor or a hydraulic actuator.

The (x, y) coordinates of the endpoint of a robot arm specify its position. These coordinates for the first and second links respectively are given in the following:

$$\begin{cases} x_1 = l_1 \cos \theta_1 \\ y_1 = l_1 \sin \theta_1 \end{cases} \tag{1}$$

$$\begin{cases} x_2 = l_1 \cos \theta_1 + l_2 \cos(\theta_1 + \theta_2) \\ y_2 = l_1 \sin \theta_1 + l_2 \sin(\theta_1 + \theta_2) \end{cases} \tag{2}$$

where l_1 and l_2 are the length of the first and second links, respectively. For the first link, kinetic energy, K_1, and potential energy, P_1, are equal to:

$$K_1 = \frac{1}{2} m_1 l_1{}^2 \dot{\theta}_1{}^2, \quad P_1 = m_1 g l_1 \sin\theta_1 \tag{3}$$

where m_1 and m_2 are the mass of the first and second links, respectively. For the velocity of the second link, v_2, the following holds:

$$v_2{}^2 = \dot{x}_2{}^2 + \dot{y}_2{}^2 = 2l_1 l_2 \left(\dot{\theta}_1{}^2 + \dot{\theta}_1 \dot{\theta}_2 \right) \cos \theta_2 + l_1{}^2 \dot{\theta}_1{}^2 + l_2{}^2 \left(\dot{\theta}_1 + \dot{\theta}_2 \right)^2 \tag{4}$$

For the second link, kinetic energy, K_2, and potential

energy, P_2, are equal to

$$K_2 = \frac{1}{2}m_2 v_2{}^2, \quad P_2 = m_2 g y_2 \qquad (5)$$

Lagrange L, is the difference between kinetic energy and potential energy. The Lagrangian motion equation of the system satisfies (6):

$$\frac{d}{dt}\frac{\partial L}{\partial \dot{q}} - \frac{\partial L}{\partial q} = \tau, \quad L = K - P \qquad (6)$$

The standard form of the dynamic of a two-link robot arm is given by (7):

$$M(q)\ddot{q} + C(q,\dot{q})\dot{q} + G(q) = \tau \qquad (7)$$

where $M(q)$ is the inertia matrix, $C(q,\dot{q})$ is a matrix including parts related to Coriolis and centripetal forces, and $G(q)$ is the gravitational vector. Similar to [17], the mathematical model of the robot arm is expressed by (8) and (9).

$$\tau_1 = m_1\left(l_1 g c_1 + l_1{}^2\ddot{\theta}_1\right) +$$
$$m_2\left(l_1{}^2\ddot{\theta}_1 + l_2{}^2\left(\ddot{\theta}_1 + \ddot{\theta}_2\right) + l_1 l_2 c_2\left(2\ddot{\theta}_1 + \ddot{\theta}_2\right) + \right. \qquad (8)$$
$$\left. l_1 g c_1 + l_2 g c_{12} - l_1 l_2 s_2 \dot{\theta}_2\left(2\dot{\theta}_1 + \dot{\theta}_2\right)\right)$$

$$\tau_2 = m_2 \times$$
$$\left(l_1 g c_{12} + l_1 l_2 c_2 \ddot{\theta}_1 + l_2{}^2\left(\ddot{\theta}_1 + \ddot{\theta}_2\right) + l_1 l_2 s_2 \dot{\theta}_1{}^2\right) \qquad (9)$$

where $c_1 = \cos\theta_1$, $c_2 = \cos\theta_2$, $s_1 = \sin\theta_1$, and $s_2 = \sin\theta_2$.
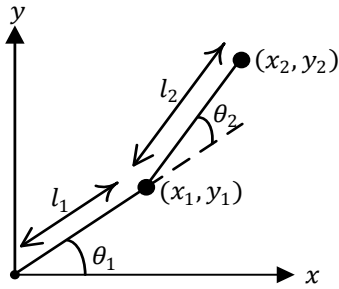

Fig. 1: Diagram of a two-link robot arm

Interval Type II Fuzzy Fractional – Order PID Controller Design

A. Fractional-Order PID Controller ($PI^\lambda D^\mu$)

The fractional-order PID controller (FOPID) was proposed in 1999. The most common FOPID is $PI^\lambda D^\mu$, and its transfer function is expressed as (10):

$$G_c(s) = K_p + \frac{K_i}{s^\lambda} + K_d s^\mu \qquad (10)$$

where λ and μ are the fractional-orders of the integral and derivative, respectively; both are real and positive. K_i, K_p, and K_d are proportional, integral and derivative gains, respectively [17], [18].

Oustaloup approximation is the most common integer-order approximation of the fractional-order element s^α in the frequency band $[\omega_L \quad \omega_H]$, according to (11):

$$s^\alpha = \omega_H^\alpha \prod_{k=-N}^{N} \frac{s-z_k}{s-p_k}, \quad 0 < \alpha < 1 \qquad (11)$$

where

$$p_k = -\omega_L\left(\frac{\omega_H}{\omega_L}\right)^{\frac{k+N+\frac{1-\alpha}{2}}{2N+1}} \quad \text{and}$$

$z_k = -\omega_L\left(\frac{\omega_H}{\omega_L}\right)^{\frac{k+N+\frac{1+\alpha}{2}}{2N+1}}$. The transfer function in (11) is proper; its relative degree is zero; its order is $2N + 1$ [19].

B. Fuzzy Fractional-Order PID Controller

In Fig. 2, the block diagram of the closed-loop system with the Fuzzy fractional-order PID (FO-FPID) controller is shown. This configuration is a combination of the Fuzzy fractional order PI and Fuzzy fractional-order PD. The inputs of the Fuzzy logic controller (FLC) are the error $(e(t))$ and its fractional derivative of order μ $(\frac{d^\mu e(t)}{dt^\mu})$. K_d and K_e are the scaling factors of the FLC inputs, and α and β are the scaling factors of the FLC outputs. The control effort, $u_{FOFPID}(t)$, is the weighted summation of the output signal of FLC, u_{FLC}, and its fractional integral of order λ as below [11]:

$$U_{FOFPID}(s) = \beta s^{-\lambda} U_{FLC}(s) + \alpha U_{FLC}(s) \qquad (12)$$

C. Interval Type II Fuzzy System

Since the membership value (or degree of membership) for the membership functions of the T1FS is deterministic, T1FS is limited in the modeling and minimizing the uncertainties [12]. The main difference between T1FS and T2FS is their membership functions. Membership functions of T2FS are Fuzzy. A type II Fuzzy set has a superior membership function and an inferior membership function; each of them can be represented by a type I Fuzzy set. The IT2FS is a special kind of T2FS with a much less calculation. The difference between T1FS and IT2FS is the membership value of the variables. It is a deterministic number in T1FS, while in IT2FS it is an interval. IT2FS is restricted from the top and bottom to the two T1FSs. They are called the UMF and the LMF, respectively. The space between the UMF and the LMF is called the footprint of uncertainty (FOU) [14].

When the accurate determination of the membership function is difficult, IT2FS is applied effectively. Researchers paid a lot of attention to IT2FS in recent years. Fig. 3 displays the configuration of the T2FS. It is shown that the only difference between the T2FS and the T1FS configuration is in the "type reduction" block. The "Fuzzification" block converts the crisp input data to a type I, type II, or singleton Fuzzy set. The block of the "Fuzzy rule base" is a set of Fuzzy if-then rules. n^{th} rule in IT2FS is represented as:

$IF\ x_1\ is\ \tilde{X}_1^n\ and\ x_2\ is\ \tilde{X}_2^n\ and\ \cdots\ and\ x_L\ is\ \tilde{X}_L^n,$
$Then\ y\ is\ \tilde{Y}^n. \qquad\qquad ,n = 1,2,\dots,N \qquad (13)$

where the superscript $\sim$ denotes the type II Fuzzy set; x_j is the input variable; $\tilde{X}_j^n$ is the type II Fuzzy set of the input; y is the output variable; $\tilde{Y}^n$ is the type II Fuzzy set

of the output; $n = 1, 2, \ldots, N$ and $j = 1, 2, \ldots, L$. N is the number of rules and L is the number of input variables. $\widetilde{Y}^n = \left[\underline{y}^n, \overline{y}^n\right]$ is an interval that is considered as the center of gravity of the IT2FS consequent. Computational steps of an IT2F are presented in Fig. 4, in which $x' = (x'_1, x'_2, \ldots, x'_L)$ is the input vector [20]. Fig. 5 and Fig. 6 display how y_l and y_r are calculated by an enhanced iterative algorithm with a stop condition (EIASC).

D. Interval Type II Fuzzy FOPID controller

The interval type II Fuzzy FOPID (IT2FO-FPID) controller is the combination of the FOPID controller and the IT2FS. IT2FO-FPID controller is used for a two-link robot arm and its optimal parameters are determined using WOA, GA and PSO optimization algorithms. The IT2FO-FPID controller based on the optimization algorithm is shown in Fig. 7.

The inputs of ith Fuzzy system are $K_{ei}e_i$ and $K_{di}(d^\mu e_i/dt^\mu)$. The optimal values of $K_{ei}, K_{di}, \mu_i, \lambda_i, \alpha_i$, and β_i are also determined using optimization algorithms. It is noteworthy that $i = 1, 2$.

In this paper, each Fuzzy controller input or output has five membership functions: Negative big (NB), negative small (NS), zero (Z), positive small (PS), and positive big (PB). The membership functions of the input and output variables for T1FS and IT2FS are shown in Fig. 8. The Fuzzy rules are given in Table 1.

Whale Optimization Algorithm

Nowadays, meta-heuristic optimization algorithms attract a lot of attention in engineering applications. They have relatively simple concepts, their implementation is easy and they do not require any problem information.

The nature-inspired meta-heuristic algorithms solve the optimization problems by imitating biological and physical phenomena.

Whale optimization algorithm (WOA) is a metaheuristic optimization algorithm inspired by the social behavior of humpback whales.

This algorithm, similar to the bubble-net hunting strategy, consists of two phases of exploration and exploitation. At the exploration stage, hunting is sought. In the exploitation phase, the hunt is encircled. Whales encircle hunting with two methods. The first method is shrinking encircling and the second method is a helix-shaped movement (spiral) to hunt and trap it [16].

The vector $\vec{A}$ is calculated as follows:

$$\vec{A} = 2\vec{a}.\vec{r} - \vec{a} \tag{14}$$

where $\vec{a}$ decreases linearly from 2 to zero through iterations, and $\vec{r}$ is a random vector in the interval $[0, 1]$.

If the random vector $\vec{A}$ is larger than 1, the algorithm enters the exploration phase.

In the exploration phase, the whales (search agents) randomly search for the prey (best solution), and the whale position, $\vec{X}$, is updated according to the position of the other whales as below:

$$\vec{X}(t + 1) = \vec{X}_{\text{rand}} - \vec{A}.\vec{D} \tag{15}$$

where t is the current iteration number, $\vec{X}_{rand}$ is a position vector chosen from population randomly and we have:

$$\vec{D} = \left|\vec{C}.\vec{X}_{rand} - \vec{X}(t)\right| \tag{16}$$

$$\vec{C} = 2.\vec{r} \tag{17}$$

In exploitation with the method of shrinking encircling, the whale position updates as follows:

$$\vec{X}(t + 1) = \overrightarrow{X^*}(t) - \vec{A}.\vec{D} \tag{18}$$

where $\overrightarrow{X^*}$ is the position of the best solution and

$$\vec{D} = \left|\vec{C}.\overrightarrow{X^*} - \vec{X}(t)\right| \tag{19}$$

By changing the values of the vectors $\vec{A}$ and $\vec{C}$, it is possible to select different points around the best solution. The value of $\vec{A}$ is random and it is in the interval $[-a, a]$. Through iterations, this interval gets smaller and the encircling radius shrinks. As a result, search agents tend toward the prey.
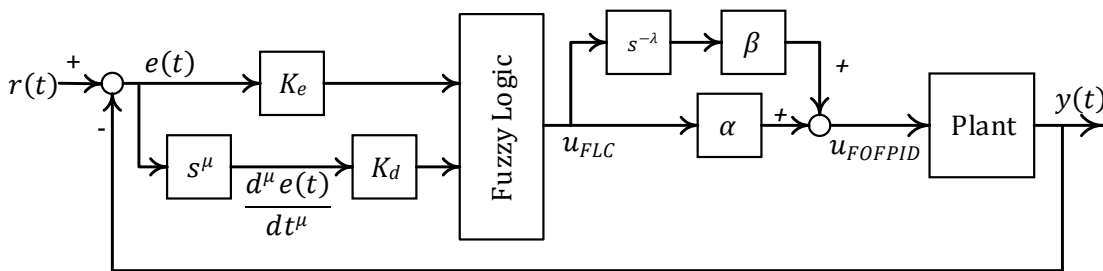

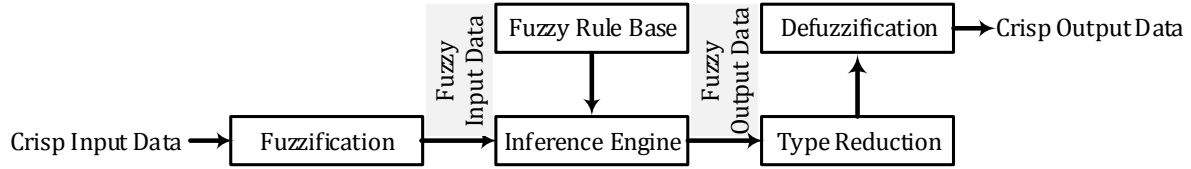Fig. 2: Block diagram of the closed-loop system with FO-FPID controller [11].
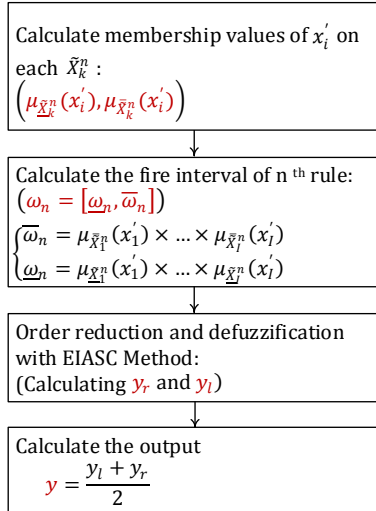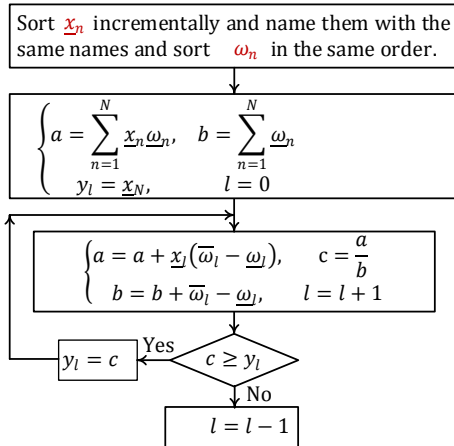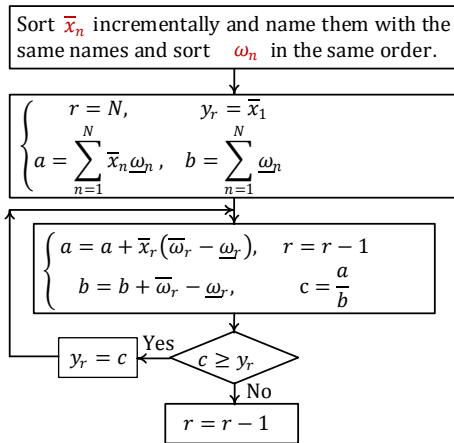
Fig. 3: The T2FS configuration.

Fig. 4: Computational steps of the IT2F.

Fig. 5: Computational steps of y_l.

Fig. 6: Computational steps of y_r.

In exploitation with the method of spiral movement, the distance between whale and prey, $\overrightarrow{D'} = \left|\overrightarrow{X^*}(t) - \vec{X}(t)\right|$, is calculated, a helix-shaped movement is formed, and the whale position is updated as follows:

$$\vec{X}(t + 1) = \overrightarrow{D'}.e^{bl}.cos(2\pi l) + \overrightarrow{X^*}(t) \quad (20)$$

where b is a constant value to define the logarithmic form of the motion and l is a random number in the interval $[-1, 1]$.

The whales swim around a prey in a circle whose radius is decreasing and along a spiral-shaped path. To model this behavior, a 50% probability in updating the whale position is assumed between the two mechanisms of shrinking encircling and spiral motion.
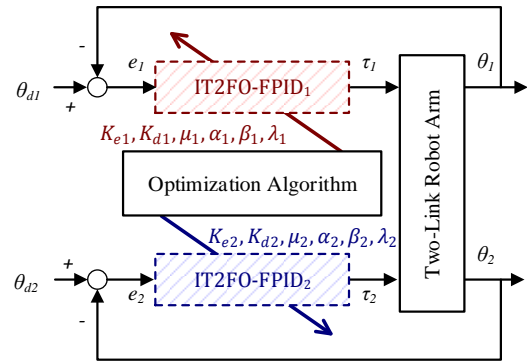

Fig. 7: Block diagram of the closed-loop two-link robot arm with IT2FO-FPID controller based on the optimization algorithm.

Table 1: Fuzzy Rules of IT2FO-FPID Controller

$K_d(d^\mu e/dt^\mu)\rightarrow$ $K_e e\downarrow$	NB	NS	Z	PS	PB
NB	NB	NB	NB	NS	Z
NS	NB	NS	NS	Z	PS
Z	NB	NS	Z	PS	PB
PS	NS	Z	PS	PS	PB
PB	Z	PS	PB	PB	PB

$$\vec{X}(t+1) =$$
$$\begin{cases} \overrightarrow{X^*}(t) - \vec{A}.\vec{D} & if \quad p < 0.5 \\ \overrightarrow{D'}.e^{bl}.cos(2\pi l) + \overrightarrow{X^*}(t) & if \quad p \geq 0.5 \end{cases} \quad (21)$$

where p is a random number in the interval $[0,1]$ [16].
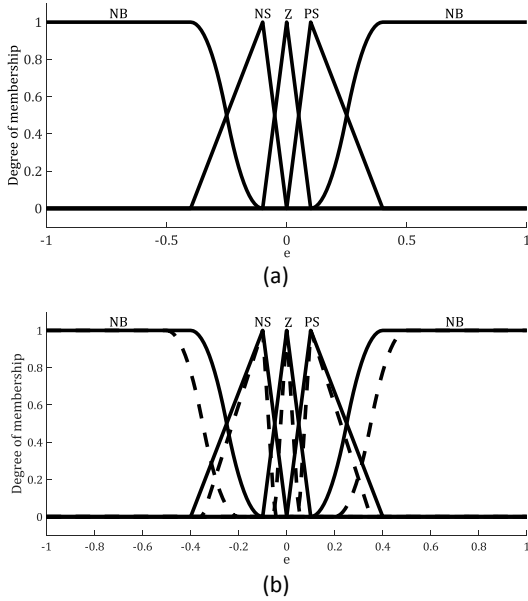
Fig. 8: Membership functions of the inputs and output, (a) T1FS, (b) IT2FS.

Simulation Results

The length and the mass of the links of the robot arm studied in this paper are as follows [17]:

$$m_1 = m_2 = 0.1 \, Kg$$
$$l_1 = 0.8 \, m, \ l_2 = 0.4 \, m \tag{22}$$

Reference inputs are as bellows:

$$\theta_{d_1} = -5.5 + 9t - 3.375t^2 + 0.375t^3$$
$$\theta_{d_2} = 13 - 12t + 4.5t^2 - 0.5t^3 \tag{23}$$

In this paper, PID, FOPID, FFOPID, and IT2FO-FPID controllers are designed. Their parameters are determined using the WOA algorithm to minimize the tracking errors with the limited control efforts (due to actuator constraints):

$$Min \quad \frac{\int_0^T |e_1(t)|dt}{T} + \frac{\int_0^T |e_2(t)|dt}{T}$$
$$subject\ to \begin{cases} |\tau_i| \le U_{max}^i \\ 0 < \lambda_i, \mu_i \le 2 \quad , i = 1,2 \\ 0 < K_{e_i}, K_{d_i}, \alpha_i, \beta_i \le 100 \end{cases} \tag{24}$$

where U_{max}^1 is the upper bound on the magnitude of the torque τ_1 and U_{max}^2 is the upper bound on the magnitude of the torque τ_2. The number of iterations in optimizing the parameters is considered identical for all the designed controllers. Fig. 9 displays the changes in the cost function value for the WOA-IT2FO-FPID controller against the iteration number. It shows a decrease in the cost function value in 200 iterations from 0.5330 to 0.1045. To compare the performance of the controllers quantitatively, the indices of the integral absolute error (IAE), integral square error (ISE), integral time absolute error (ITAE) and integral time square error (ITSE) are used:

$$IAE = \frac{\int_0^T |e_1(t)|dt}{T} + \frac{\int_0^T |e_2(t)|dt}{T} \tag{25}$$

$$ISE = \frac{\int_0^T e_1{}^2 dt}{T} + \frac{\int_0^T e_2{}^2 dt}{T} \tag{26}$$

$$ITA = \frac{\int_0^T t|e_1(t)|dt}{T} + \frac{\int_0^T t|e_2(t)|dt}{T} \tag{27}$$

$$ITSE = \frac{\int_0^T te_1{}^2 dt}{T} + \frac{\int_0^T te_2{}^2 dt}{T} \tag{28}$$

Fig. 10 shows the position of the robot controlled by the above-mentioned controllers, Fig. 11 displays their tracking error, and Fig. 12 shows control efforts. Error conflicts with control effort. Using the proposed control design, an acceptable trade-off is made between error and control signal. Table 2 compares the values of IAE, ISE, ITAE and ITSE indices for them. The IAE and ISE indices are good indexes to assess the quality of the transient response, and the ITAE and ITSE indices are appropriate evaluating indexes for the quality of the steady-state response. Qualitative and quantitative analyses confirm that IT2FO-FPID, FFOPID, FOPID, and PID controllers have superior performance in both transient and steady-state, respectively.

To evaluate the performance of the WOA algorithm, the parameters of the IT2FO-FPID controller are determined with WOA, PSO, and GA algorithms. The parameters of the controllers are compared in Table 3. To compare fairly and rationally, the number of iterations and the initial random population are considered the same for them. The performance of the controlled robot is compared in Table 4 with the quantitative indices (25)-(28). The position of the robot controlled by these controllers, their tracking error and their control effort are displayed in Fig. 13 to Fig. 15, respectively. Qualitative and quantitative analyses confirm that WOA is comparable to GA and PSO. The results demonstrate the superior performance of WOA- IT2FO-FPID.

A. Robustness of the Controller

The parameters uncertainties and external disturbances have inappropriate effects on the performance. To evaluate the robustness of the proposed controller, the controller performance is investigated despite the input disturbances and variations of the important parameters of the model.

Disturbance Effect: the robustness of the proposed controller against disturbances is investigated by adding external disturbances to the output of the proposed controller. External disturbances are applied according to Table 5. Indices (25)-(28) for controllers WOA-PID, WOA-FOPID, WOA-FFOPID, and WOA-IT2FO-FPID are compared in Table 5. As can be seen, the WOA-IT2FO-FPID controller has the smallest and the slightest variation for the indices (25)-(28) compared to the other control structures. This controller performs more robust than other controllers despite input disturbance. The two-link robot arm controlled by the WOA-IT2FO-FPID controller tracks the desirable path with much less error.

The results demonstrate the robustness and better

performance of this controller in comparison to the other controllers.

Parameter variations Effect: 6 changes in two important parameters of mass and length of the links of the robot arm (m_i, l_i, for $i = 1,2$) are considered. Applying 5% variation in the mass and length of the links of the robot arm, the indices (25)-(28) are compared in Tables 6 and 7 for the WOA-PID, WOA-FOPID, WOA-FFOPID and WOA-IT2FO-FPID controllers. Despite the

parameter uncertainties, for the WOA-IT2FO-FPID controller the tracking error is retained in an acceptable range and the control performance is still acceptable. For the WOA-IT2FO-FPID controller compared to the other controllers, indices (25)-(28) are the smallest and variations of the indices (25) and (26) are smaller and smaller.

In other words, the WOA-IT2FO-FPID controller performs more robust than the other controllers.
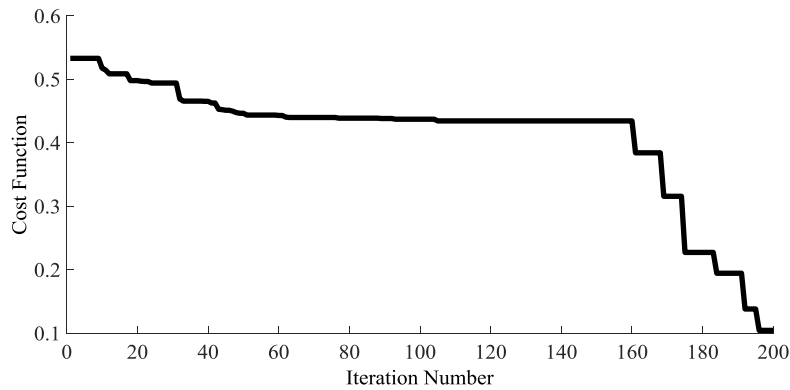

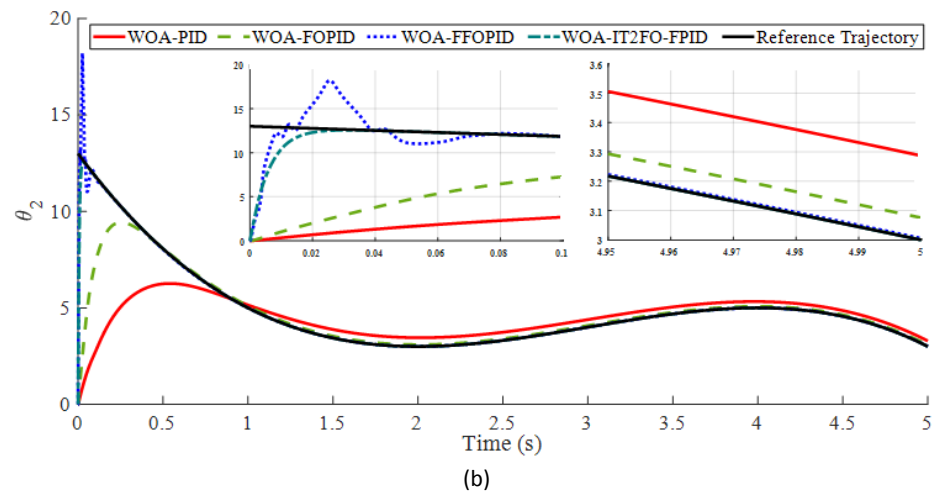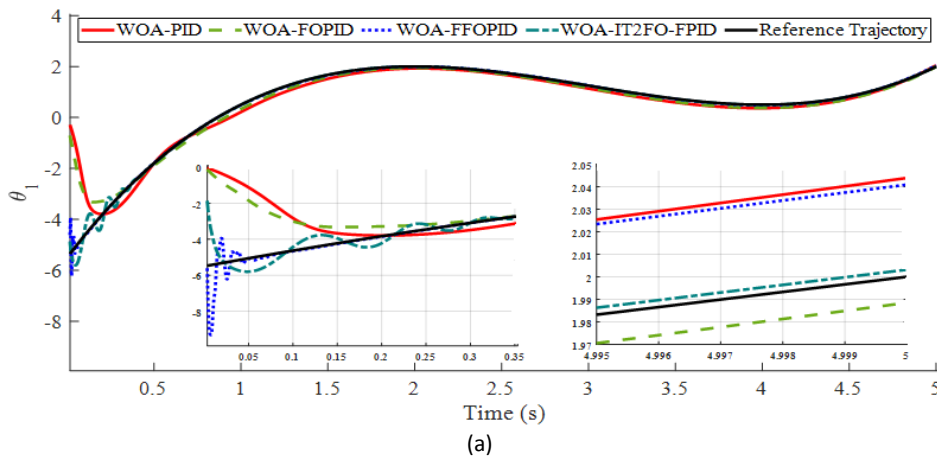Fig. 9: Variations of the cost function value through iterations for the WOA-IT2FO-FPID controller.

(a)

(b)

Fig. 10: Robot position in tracking the reference inputs for different WOA-optimized controllers, (a) θ_1, (b) θ_2.
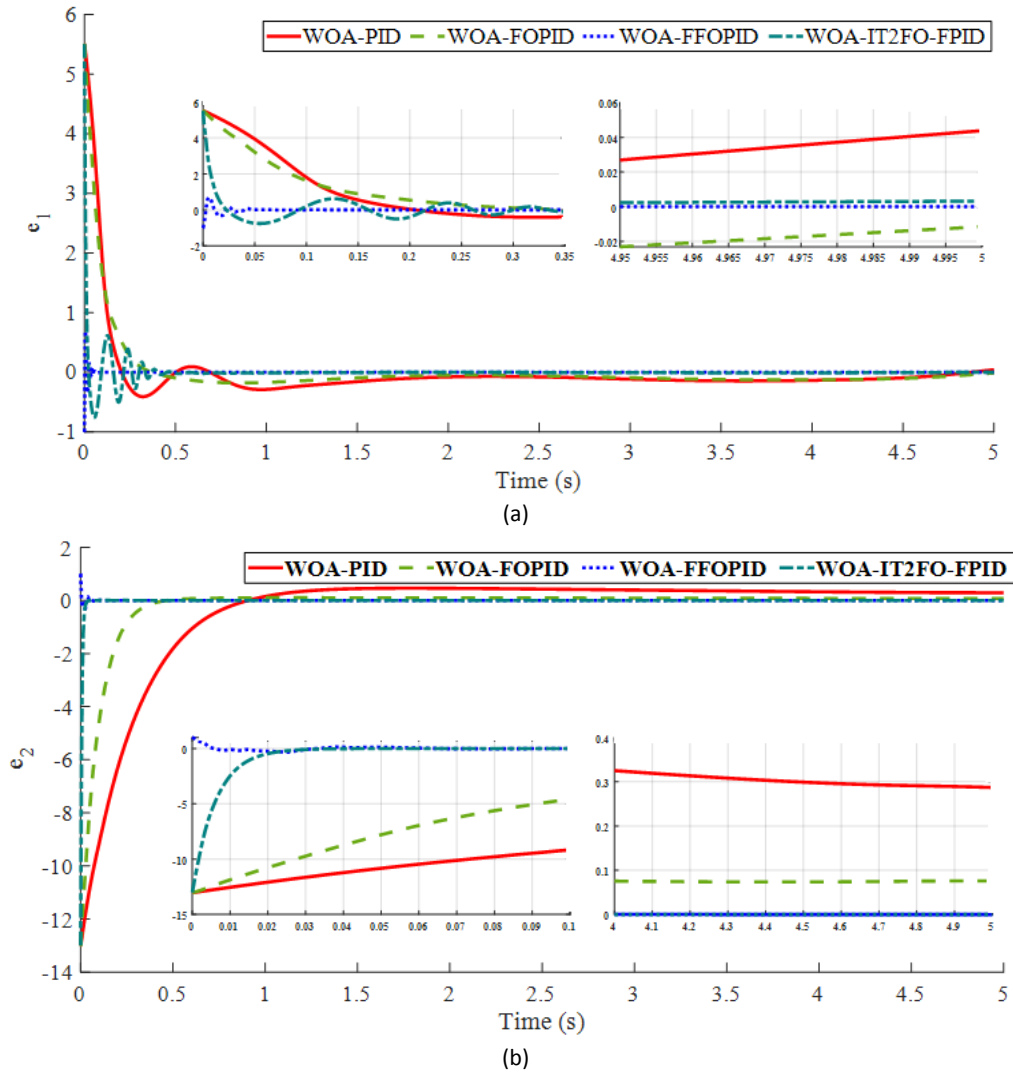
Fig. 11: Tracking error for different WOA-optimized controllers, (a) e_1, (b) e_2 .

Table 2: Quantitative comparison of the performance of different controllers optimized with WOA

index→ Controller↓	IAE	ISE	ITAE	ITSE
WOA-PID	1.6600	9.5641	1.1963	0.9953
WOA-FOPID	1.2720	9.2171	0.4561	0.2000
WOA-FFOPID	0.4444	3.2550	0.0418	0.0091
WOA-IT2FO-FPID	0.1045	0.4877	0.0175	0.0024

Conclusion

In this paper, the interval type II fractional-order fuzzy proportional integral derivative controller (IT2FO- FPID) was designed to control the two-link robot arm. The controller parameters were optimized using the Whale optimization algorithm (WOA). The quantitative and qualitative results of the simulations demonstrated that the controller performance improves with the WOA-based IT2FO-FPID controller compared to controllers with similar-structures whose parameters were optimized with the WOA considering the limited control effort.

The performance of the IT2FO-FPID controller whose parameters were optimized using WOA, GA, and PSO were compared. The quantitative and qualitative results of the simulations confirmed that the superior parameter determination is about the WOA. For fair evaluation, the number of iterations was chosen the same in comparisons. Sensitivity analyses demonstrated the robust performance of the proposed control structure.
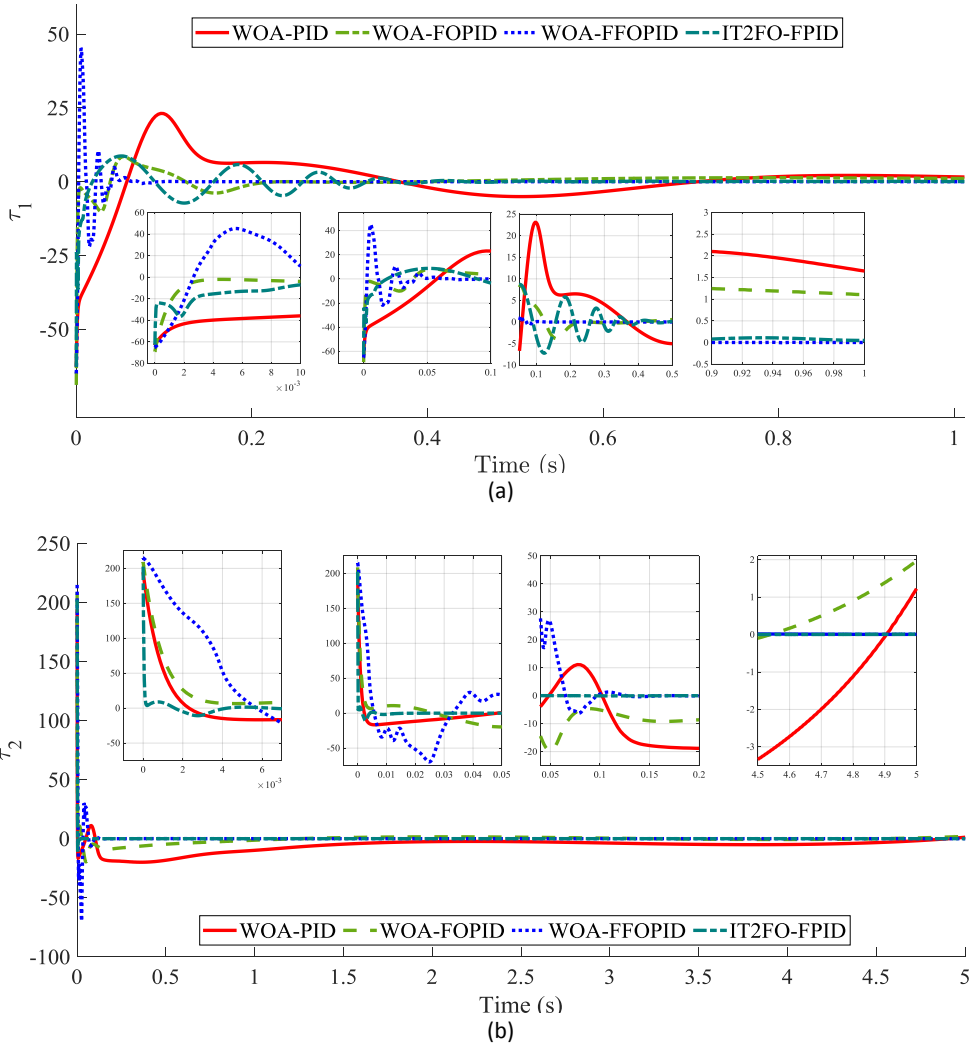
Fig. 12: Control effort for different WOA-optimized controllers, (a) τ_1, (b) τ_2.

Table 3: Parameters of IT2FO-FPID controllers optimized with different algorithms

Parameters→ Controller↓	K_{e_1}	K_{d_1}	α_1	β_1	μ_1	λ_1	K_{e_2}	K_{d_2}	α_2	β_2	μ_2	λ_2
GA-IT2FO-FPID	15	21.71	6.65	0.21	1.38	0.91	37.8	0.64	58.35	6.11	0.96	1.01
PSO-IT2FO-FPID	17.03	19.75	8.12	0.26	0.92	1.12	43.9	0.59	68.73	6.9	1.3	0.92
WOA-IT2FO-FPID	27	8.5	10.4	1	0.89	1.05	30.1	0.6	80.13	18.4	1.67	0.94

Table 4: Quantitative comparison of performance of IT2FO-FPID controllers optimized with different algorithms

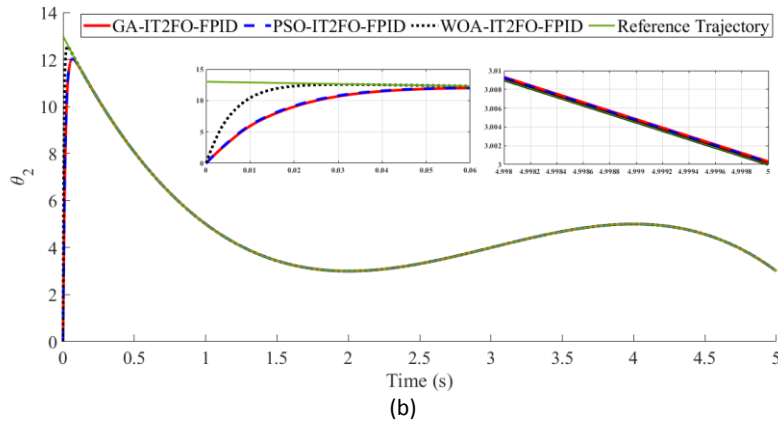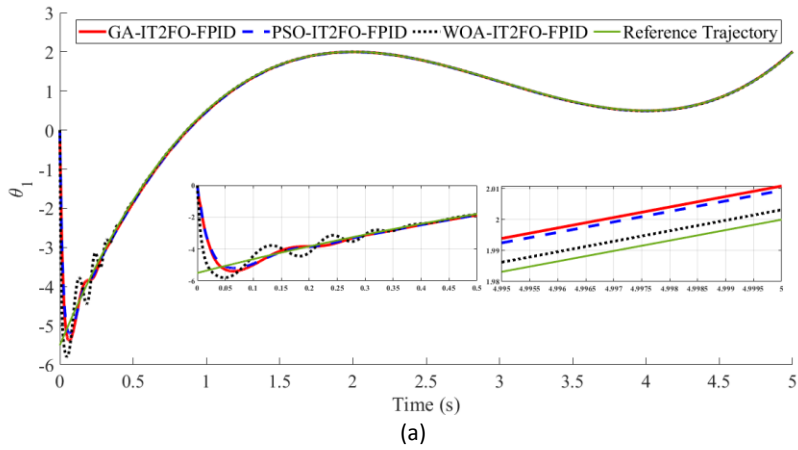| Index→ Controller↓	*IAE*	*ISE*	*ITAE*	*ITSE*
GA-IT2FO-FPID	0.1988	1.3378	0.0235	0.0051
PSO-IT2FO-FPID	0.1815	1.2087	0.0257	0.0046
WOA-IT2FO-FPID	0.1045	0.4877	0.0175	0.0024

(a)

(b)

Fig. 13: Robot position in tracking the reference inputs for IT2FO-FPID controller optimized with different algorithms, (a) θ_1, (b) θ_2.
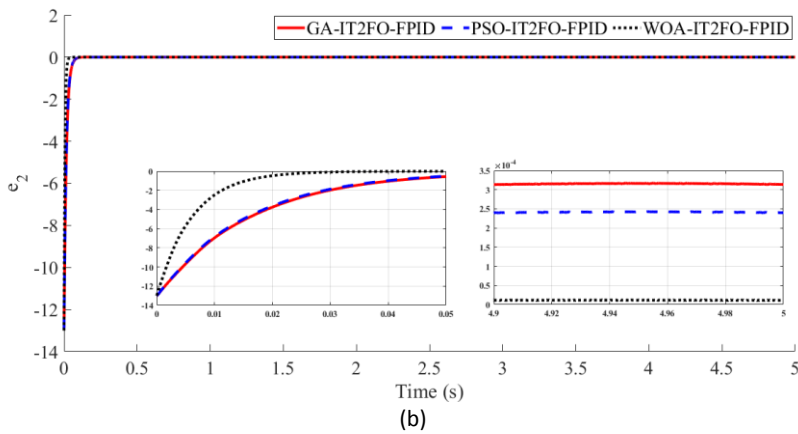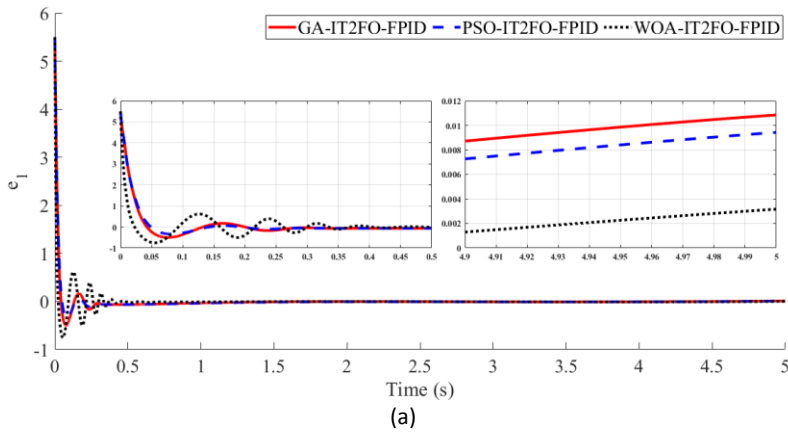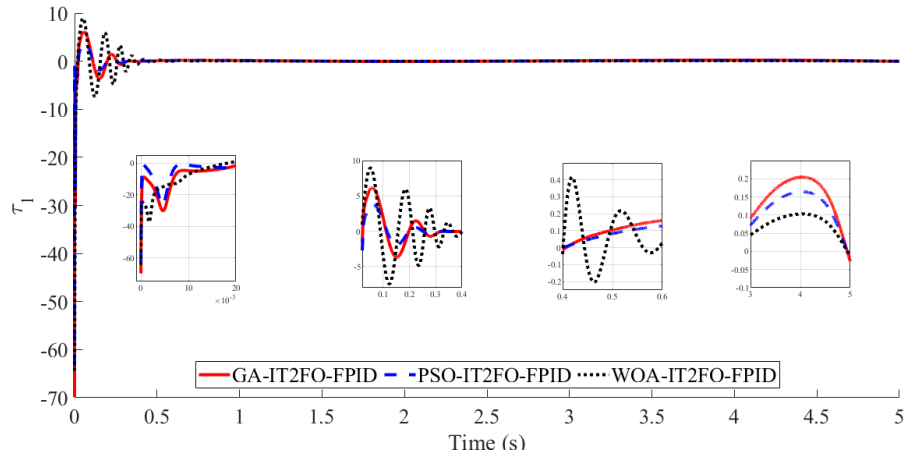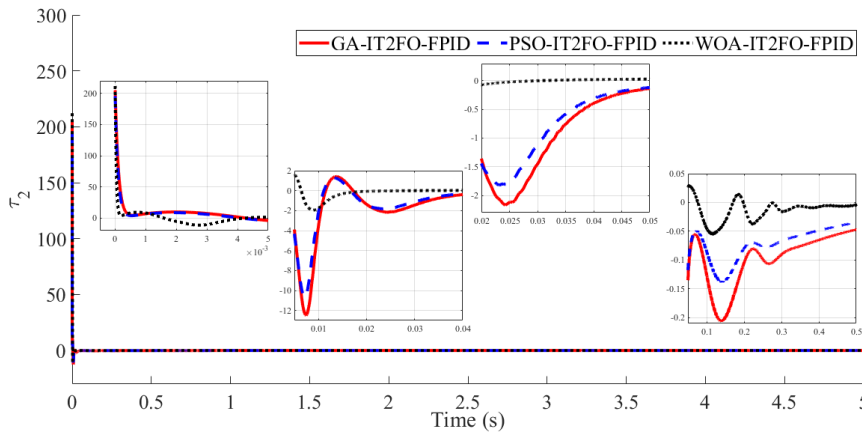

(a)

(b)

Fig. 14: Tracking error for IT2FO-FPID controller optimized with different algorithms (a) e_1, (b) e_2.

Table 5: Quantitative comparison of the robust performance of different controllers optimized by WOA against the input disturbance

		Nominal condition	First link $0.1\,sin(50t)$	First link $1\,sin(50t)$	Second link $0.1\,sin(50t)$	Second link $1\,sin(50t)$	Both links $0.1\,sin(50t)$	Both links $1\,sin(50t)$
WOA-IT2FO-FPID	ITSE	0.002	0.002	0.002	0.002	0.002	0.002	0.003
	ITAE	0.018	0.017	0.017	0.018	0.018	0.018	0.025
	ISE	0.488	0.488	0.488	0.488	0.488	0.488	0.488
	IAE	0.105	0.105	0.105	0.105	0.105	0.105	0.106
WOA-FFPID	ITSE	0.009	0.009	0.009	0.009	0.009	0.009	0.009
	ITAE	0.042	0.042	0.042	0.042	0.045	0.042	0.045
	ISE	3.255	3.255	3.261	3.255	3.252	3.252	3.232
	IAE	0.444	0.444	0.445	0.445	0.445	0.444	0.443
WOA-FOPID	ITSE	0.200	0.201	0.201	0.191	0.163	0.163	0.169
	ITAE	0.456	0.458	0.458	0.458	0.475	0.475	0.469
	ISE	9.217	9.254	9.254	8.674	6.878	6.878	7.281
	IAE	1.272	1.276	1.276	1.207	0.998	0.998	1.044
WOA-PID	ITSE	0.995	1.010	1.010	1.008	0.921	0.921	0.936
	ITAE	1.196	1.199	1.199	1.198	1.242	1.242	1.232
	ISE	9.564	9.619	9.619	9.442	7.917	7.917	8.113
	IAE	1.66	1.671	1.671	1.652	1.463	1.463	1.49

(a)

(b)

Fig. 15: Control effort for IT2FO-FPID controller optimized with different algorithms, (a) τ_1, (b) τ_2.

Table 6: Quantitative comparison of robust performance of different controllers optimized by WOA against 5% increase and decrease in Mass of the links of the robot arm.

		Nominal condition	Increase m_1	Decrease m_1	Increase m_2	Decrease m_2	Both increase	Both decrease
WOA-IT2FO-FPID	*ITSE*	0.002	0.002	0.002	0.003	0.002	0.003	0.002
	ITAE	0.018	0.018	0.017	0.018	0.017	0.018	0.017
	ISE	0.488	0.489	0.486	0.502	0.474	0.503	0.473
	IAE	0.105	0.105	0.104	0.107	0.102	0.108	0.101
WOA-FFOPID	*ITSE*	0.009	0.01	0.011	0.012	0.009	0.010	0.014
	ITAE	0.042	0.050	0.074	0.047	0.052	0.044	0.095
	ISE	3.255	3.344	3.298	3.479	3.208	3.406	3.237
	IAE	0.444	0.465	0.477	0.491	0.447	0.471	0.503
WOA-FOPID	*ITSE*	0.200	0.20	0.20	0.205	0.195	0.205	0.195
	ITAE	0.456	0.458	0.455	0.459	0.454	0.46	0.452
	ISE	9.217	9.209	9.206	9.443	8.96	9.448	8.945
	IAE	1.272	1.271	1.271	1.299	1.241	1.299	1.240
WOA-PID	*ITSE*	0.995	1.028	1.025	1.028	1.023	1.033	1.023
	ITAE	1.196	1.202	1.195	1.197	1.197	1.203	1.194
	ISE	9.564	9.821	9.728	9.912	9.714	10.01	9.668
	IAE	1.66	1.694	1.686	1.708	1.678	1.718	1.675

Table 7: Quantitative comparison of robust performance of different controllers optimized by WOA against 5% increase and decrease in length of the links of the robot arm.

		Increase l_1	Decrease l_1	Increase l_2	Decrease l_2	Both increase	Both decrease
WOA-IT2FO-FPID	*ITSE*	0.003	0.002	0.002	0.002	0.003	0.002
	ITAE	0.019	0.017	0.018	0.018	0.019	0.017
	ISE	0.51	0.468	0.468	0.468	0.51	0.468
	IAE	0.114	0.097	0.105	0.105	0.114	0.097
WOA-FFOPID	*ITSE*	0.012	0.019	0.009	0.009	0.012	0.019
	ITAE	0.047	0.115	0.042	0.042	0.047	0.115
	ISE	3.476	3.247	3.255	3.255	3.476	3.247
	IAE	0.487	0.528	0.444	0.444	0.487	0.528
WOA-FOPID	*ITSE*	0.204	0.196	0.200	0.200	0.204	0.196
	ITAE	0.458	0.455	0.456	0.456	0.458	0.455
	ISE	9.398	8.994	9.217	9.217	9.398	8.994
	IAE	1.293	1.247	1.272	1.272	1.293	1.247
WOA-PID	*ITSE*	1.041	1.013	0.995	0.995	1.041	1.013
	ITAE	1.200	1.196	1.196	1.196	1.200	1.196
	ISE	9.988	9.521	9.564	9.564	9.988	9.521
	IAE	1.719	1.658	1.660	1.660	1.719	1.658

Author Contributions

M. Vaghefi collected and reviewed the related papers to choose the appropriate model. F. Jamshidi searched the control schemes to choose the suitable one. M. Vaghefi investigated the recent intelligent optimization methods. F. Jamshidi carried out the simulation and interpreted the results. F. Jamshidi wrote the manuscript and M. Vaghefi polish it.

Acknowledgment

Conflict of Interest

The author declares that there is no conflict of interest regarding the publication of this manuscript. In addition, the ethical issues, including plagiarism, informed consent, misconduct, data fabrication and/or falsification, double publication and/or submission, and redundancy have been completely observed by the authors.

Abbreviations

IT2FO-FPID Interval Type II Fuzzy Fractional-Order Proportional Integral Differential

WOA	Whale Optimization Algorithm
FOPID	Fractional-Order PID
PID	Proportional Integral Derivative
SMC	Sliding Mode Controller
PSO	Particle Swarm Optimization
CSA	Cuckoo Search Algorithm
T1FS	Type I Fuzzy System
T2FS	Type II Fuzzy System
ABC	Artificial Bee Colony
IT2FS	Interval Type II Fuzzy System
FO-FPID	Fuzzy Fractional-Order PID
FOU	Footprint of Uncertainty
EIASC	Enhanced Iterative Algorithm with a Stop Condition
IAE	Integral Absolute Error
ISE	Integral Square Error
ITAE	Integral Time Absolute Error
ITSE	Integral Time Square Error

References

[1] A. Nourollah, N. Behzadpour, "Robot arm reconfiguration to minimization moving parts," Journal of Electrical and Computer Engineering Innovations, 6(2): 227-242, 2018.

[2] R. Sharma, P. Gaur, A. Mittal, "Design of two-layered fractional-order Fuzzy logic controllers applied to robotic manipulator with variable payload," Applied Soft Computing, 47): 565-576, 2016.

[3] C. Hang, K. Astrom, W. Ho, "Refinements of the ziegler-nichols tuning formula," IEE Proceedings D-Control Theory and Applications, 138(2): 111-118, 1991.

[4] S. Sharouni, P. Naderi, N. Taghizadegan, "Driving/regeneration and stability enhancement of a 4wd hybrid vehicles using multi-stage Fuzzy controller," Journal of Electrical and Computer Engineering Innovations, 1(1): 35-42, 2013.

[5] J. L. Meza, V. Santibáñez, R. Soto, and M. A. Liama, "Fuzzy self-tuning PID semiglobal regulator for robot manipulators," IEEE Transactions on Industrial Electronics, 59(6): 2709-2717, 2012.

[6] A. Kumar, V. Kumar, "Evolving an interval type-2 Fuzzy PID controller for the redundant robotic," Expert Systems with Applications, 73: 161-177, 2017.

[7] J. Mukherjee, S. Mukherjee, I. Narayan Kar, "Sliding mode control of planar snake robot with uncertainty using virtual holonomic constraints," IEEE Robotics and Automation Letters, 2(2): 1077-1084, 2017.

[8] S. Massou, I. Boumhidi, "Optimal neural network-based sliding mode adaptive control for two-link robot," International Journal of Systems, Control and Communications, 8(3): 204-216, 2017.

[9] I. Podlubny, "Fractional-order systems and PID-controllers, " IEEE Trans Automatic Control, 44(1): 208-214, 1999.

[10] R. Sharma, P. Gaur, A. Mittal, "Performance analysis of two-degree of freedom fractional-order PID controllers for robotic manipulator with payload," ISA Transaction, 58: 279-291, 2015.

[11] S. Das, I. Pan, A. Gupta, "A novel fractional-order Fuzzy PID controller and its optimal time domain tuning based on integral performance indices," Engineering Applications of Artificial Intelligence, 25(2): 430-442, 2012.

[12] Y. Arya, N. Kumar, "BFOA-scaled fractional-order Fuzzy PID controller applied to AGC of multi- area multi-source electric power generating systems," Swarm and Evolutionary Computation, 32: 202-218, 2016.

[13] R. Sharma, P. Gaur, A. Mittal, "Optimum design of fractional-order hybrid Fuzzy logic controller for a robotic manipulator," Arabian Journal for Science and Engineering, 42(2): 739-750, 2017.

[14] A. Kumar, V. Kumar, "A novel interval type-2 fractional-order Fuzzy PID controller: Design, performance evaluation, and its optimal time domain tuning," ISA Transaction, 68: 251-275, 2017.

[15] R. Sharma, K. Rana, V. Kumar, "Performance analysis of fractional-order Fuzzy PID controllers applied to a robotic manipulator," Expert Systems with Applications, 41(9): 4274-4289, 2014.

[16] S. Mirjalili, A. Lewis, "The Whale optimization algorithm," Advances in Engineering Software, 95: 51-67, 2016.

[17] A. Kumar, V. Kumar, "Hybridized ABC-GA optimized fractional-order Fuzzy pre-compensated FOPID control design for 2-DOF robot manipulator," AEU - International Journal of Electronics and Communications, 79: 219-233, 2017.

[18] C. Muresan, C. Ionescu, S. Folea, R. D. Ke, "Fractional-order control of unstable processes: the magnetic levitation study case," Nonlinear Dynamics, 80: 1761-1772, 2015.

[19] I. Pan, S. Das, "Fractional-order load-frequency control of interconnected power systems using chaotic multi- objective optimization," Applied Soft Computing, 29: 328-344, 2015.

[20] Y. Chen, D. Wang, W. Ning, "Studies on centroid type-reduction algorithms for general type-2 Fuzzy logic systems," Int. J. Innovative Comput., Inf. Control, 11(6): 1987-2000, 2015.

Biographies

Fatemeh Jamshidi, received her B.Sc. degree in Biomediacl Engineering (2002) from Ahvaz Jundishapur University of Medical Sciences, and M.Sc. and Ph.D. degrees in Control Engineering from Shiraz University (2005) and Tarbiat Modares University (2011), respectively. She is an Assistant Professor in Fasa University and her research interests are Robust Control, Robotic, Fuzzy systems, Control of power systems and artificial intelligence.

Mahsa Vaghefi, received her B.Sc. degree in Electrical Engineering (2004) from Shariati Technical University, and M.Sc. and Ph.D. degrees in Biomedical Engineering from Shahed University (2008) and IAU, Tehran Science and Research Branch (2015), respectively. She is an Assistant Professor in IAU, Shiraz Branch and her research interests are signal processing, nonlinear dynamics, and artificial intelligence.